Bioorganic & Medicinal Chemistry 16 (2008) 10338–10344

Contents lists available at ScienceDirect

Bioorganic & Medicinal Chemistry

journal homepage: www.elsevier.com/locate/bmc

Dimer of 2,7-diamino-1,8-naphthyridine for the detection of mismatches formed by pyrimidine nucleotide bases

Akio Kobori [a], Kazuhiko Nakatani [b,*]

[a] Department of Biomolecular Engineering, Graduate School of Science and Technology, Kyoto Institute of Technology, Matsugasaki, Sakyo-ku, Kyoto 606-8585, Japan
[b] Department of Regulatory Bioorganic Chemistry, The Institute of Scientific and Industrial Research, Osaka University, 8-1 Mihoga-oka, Ibaraki 567-0047, Japan

ARTICLE INFO

Article history:
Received 22 September 2008
Revised 11 October 2008
Accepted 14 October 2008
Available online 17 October 2008

Keywords:
Mismatched base pair
SPR
Naphthyridine

ABSTRACT

Discrimination of base mismatches from normal Watson–Crick base pairs in duplex DNA constitutes a key approach to the detection of single nucleotide polymorphisms (SNPs). We have developed a sensor for a surface plasmon resonance (SPR) assay system to detect G–G, A–A, and C–C mismatch duplexes by employing a surface upon which mismatch-binding ligands (MBLs) are immobilized. We synthesized a new MBL consisting of 2,7-diamino-1,8-naphthyridine (damND) and immobilized it onto a CM5 sensor chip to carry out the SPR assay of DNA duplexes containing a single-base mismatch. The SPR sensor with damND revealed strong responses to all C–C mismatches, and sequence-dependent C–T and T–T mismatches. Compared to ND- and naphthyridine-azaquinolone hybrid (NA)-immobilized sensor surfaces, with affinity to mismatches composed of purine nucleotide bases, the damND-immobilized surface was useful for the detection of the mismatches composed of pyrimidine nucleotide bases.

1. Introduction

Now that human genome sequencing has been accomplished, the search for and use of single nucleotide polymorphisms (SNPs) responsible for certain types of disease risk become central topics of investigation in genomic science for the prevention and the diagnosis of the diseases.[1–6] The discrimination between mutated and wild-type sequences has been achieved by direct sequencing[7–9] and observation of differences in responses to probe DNA.[10–25] Typical methods used for direct sequencing include single-primer extension[26,27] and allele-specific PCR.[28–33] The methods belonging to the latter category employ techniques based on the hybridization of allele-specific probes. Direct sequencing relies on the fidelity of DNA polymerase, whereas allele-specific hybridization is based on the relatively low thermal stability of mismatched duplexes compared to that of fully matched duplexes. Another SNPs typing method is heteroduplex analyses, which determines the presence of SNPs in testing sample DNAs by detecting the mismatched base pairs in heteroduplex produced between sample and the standard DNAs.[34–36] Our group has taken a modified approach to discriminating between mismatched duplexes and fully matched duplexes by selectively increasing the thermal stability of the mismatched duplexes.[37–42] Small molecular ligands that selectively bind to mismatched base pairs, with discrimination of the nucleotide bases that comprise the mismatch, have been designed and synthesized. These mismatch-binding ligands (MBLs) were shown to stabilize specific mismatched base pairs by selective binding. On the surface of a surface plasmon resonance (SPR) sensor, MBLs were covalently immobilized, prepared, and used for the detection of target mismatched base pairs. The SPR assays with MBL immobilized sensors for the detection of mismatches are simple in operation, rapid and accurate in analysis, and low in cost, whereas conventional heteroduplex analyses which require chemical and enzymatic cleavages at the mismatched site,[43] or selective capture with mismatch-binding proteins[44] applied to low-throughput screening. The MBL-SPR sensors successfully detected duplexes containing mismatched base pairs in the range below 10 nM.[45]

Several issues became apparent in the course of studies using MBL-SPR sensors. One major issue has been the low affinity of MBLs for mismatches composed of pyrimidine nucleotide bases, especially those containing a thymine base. To recognize thymine, 2,6-diaminopyridine was the choice among heterocycles due to its complementary hydrogen-bonding surface.[45] We synthesized MBLs consisting of 2,6-diaminopyridine with the expectation of an affinity for mismatches composed of thymine; however, these attempts were not successful. In our previous studies, we found that MBLs composed of *N*-alkyl-2-amino-1,8-naphthyridine (amND) strongly bound to C–C mismatched base pairs (Fig. 1).[46] The C-selective binding of amND was rationalized by facile protonation at the N1 ring nitrogen of the 1,8-naphthyridine heterocycle in amND under neutral pH to produce a hydrogen-bonding surface fully complementary to that of the cytosine. In fact, the binding of amND to the C–C mismatch was markedly suppressed in solutions with pH values higher than the pK_a (6.8) of the protonated amND.

* Corresponding author. Tel./fax: +81 6 6879 8455.
E-mail address: nakatani@sanken.osaka-u.ac.jp (K. Nakatani).

0968-0896/$ - see front matter © 2008 Published by Elsevier Ltd.
doi:10.1016/j.bmc.2008.10.035

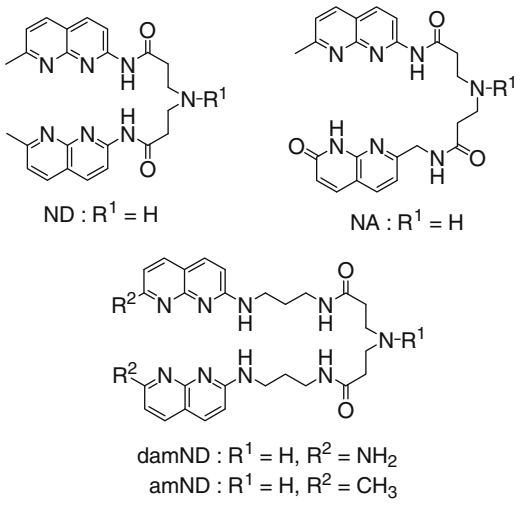

Figure 1. Structures of mismatch binding ligands. R1=$(CH_2)3NHCO(CH_2)3NH_2$ for immobilization to the surface.

The SPR sensor with amND on the surface showed marked binding to duplexes containing C–C mismatches and moderate binding to those containing C–T mismatches. The observed binding of amND to C–T mismatches was thought to be due to protonation at the N8 ring nitrogen of the 1,8-naphthyridine heterocycle, thus producing a hydrogen-bonding surface fully complementary to that of thymine.

In the course of related studies on molecular binding to a single-nucleotide bulge, we found that *N,N'*-dialkyl-2,7-diamino-1,8-naphthyridine bound not only to C bulges but also to T bulges, with comparable affinity.[47] The improved binding of 2,7-diamino-1,8-naphthyridine compared to that of 2-amino-7-methyl-1,8-naphthyridine to thymine could be accounted for by a polymorphic nature of the protonated form of 2,7-diamino-1,8-naphthyridine in terms of hydrogen bonding to both cytosine and thymine bases (Fig. 2). With the results of previous studies in mind, we synthesized a second-generation MBL consisting of 2,7-diamino-1,8-naphthyridine for the detection of mismatches containing pyrimidine nucleotide bases. The 2,7-diamino-1,8-naphthyridine dimer (damND)-equipped sensor surface revealed strong SPR responses to duplexes with a C–C mismatch. The SPR sensor with the parent MBL amND was more sensitive to base pairs flanking C–C mismatches than the damND-immobilized sensor. Furthermore, the damND-sensor showed SPR responses to all C–T and T–T mismatches. The results described here demonstrate that when immobilized on an SPR sensor surface, damND is a useful molecule for detecting C–C, C–T, and T–T mismatches.

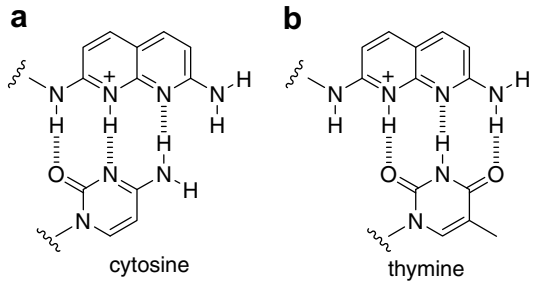

Figure 2. Plausible hydrogen bonding between the protonated 2,7-diamino-1,8-naphthyridine with (a) cytosine and (b) thymine.

2. Results and discussion

2.1. Preparation of diaminonaphthyridine dimer (damND)

The synthesis of damND **1** was straightforward, as shown in Scheme 1. *N*-Acetyl-2-amino-7-chloro-1,8-naphthyridine[48,49] was reacted with *N*-Boc-1,3-diaminopropane to give *N*-alkyl-2,7-diamino-1,8-napthyridine derivative **2**. Deprotection of the Boc group of **2** followed by coupling with *N*-Boc-3,3-iminobis(pentafluorophenyl proionate) provided the *N*-Boc-protected damND **4**. Removal of the Boc protecting group of the secondary amino group of **4** afforded the synthesis of damND **1**. To immobilize damND onto a gold surface, the secondary amino group in the linker connecting two naphthyridine heterocycles was tethered to a short linker by a reductive amination with 4-((*tert*-butoxy)carbonylamino)-*N*-(3'-oxopropyl)butanamide to give **5**, the chemical identity of which was fully characterized by ^{1}H NMR, ^{13}C NMR, and high-resolution FAB mass spectrometry. Finally, the Boc group at the primary amino group of **5** was removed to give the damND derivative **6**, which was then prepared for immobilization on the sensor surface with the carboxyl group.

2.2. Preparation of MBL-SPR sensors

The damND derivative **6** was immobilized on the carboxymethyl dextran surface of a commercially available CM5 sensor chip (BIAcore)[50,51] after activation of the carboxyl group on the surface with *N*-hydroxysuccinimide according to the manufacturer's protocol. In addition to damND, two previously characterized MBLs (ND, which binds to G–G mismatches,[37] and NA, which binds to A–A mismatches[41]) were also immobilized on the surface in a different flow channel on the same sensor chip. Thus, the DNA samples were simultaneously analyzed by three MBL-immobilized surfaces, enabling rapid and reliable comparison of the three MBL surfaces in terms of binding affinity, selectivity, and complimentary character. The amount of MBL immobilized on the surface was deter-

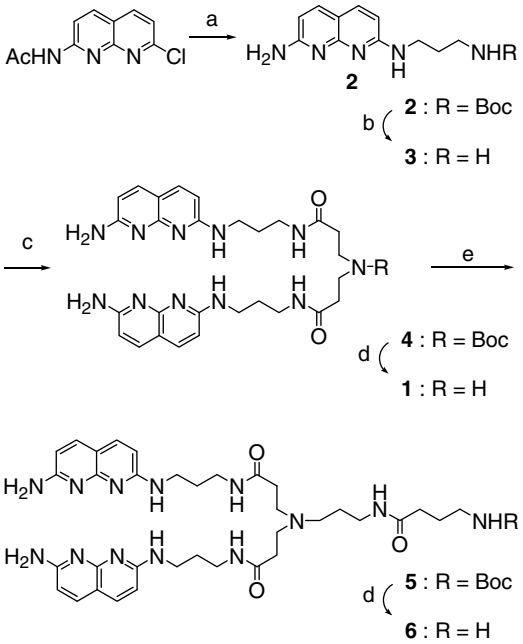

Scheme 1. Reagents and conditions: (a) *N*-Boc-1,3-propanediamine, $CHCl_3$, 120 °C (in a sealed tube), 2 days, 58%; (b) 4 N HCl in EtOAc, $CHCl_3$ 98%; (c) *N*-Boc-3,3-iminobis(pentafluorophenyl propionate), DMSO, 79%; (d) 4 N HCl in EtOAc, MeOH; (e) 4-(*tert*-butoxycarobnylamino)-*N*-(3'-oxopropyl)butanamide, $NaBH_3CN$, MeOH, 71% (from **4**).

```
5'-d(GTT ACA GAA TCT X N Y  AAG CCT AAT ACG)-3'
3'-d(CAA TGT CTT AGA Y'N X' TTC GGA TTA TGC)-5'
```

Chart 1. The sequence of DNA duplexes used for SPR analyses. N–N' is the mismatched base pair flanked by Watson–Crick base pairs of X–Y' and Y–X'.

mined based on the SPR intensity before and after MBL immobilization as follows: ND, 338 response units (RU); NA, 710 RU; and damND, 621 RU.

2.3. DNA samples for SPR analyses

We used 27-mer DNA duplexes containing a single mismatched site in the middle of the duplex for the SPR analyses with the three-MBL sensor. Our previous studies have shown that MBL-binding to the mismatches was affected by the base pairs flanking the mismatch.[37,42,47] DNA foot-printing analyses revealed that ND-binding to G–G mismatches was favorable for those sites flanked by G–C base pairs.[37] Thermal denaturation studies demonstrated that NA-binding to A–A mismatches was highly sequence-dependent.[41] The A–A mismatch in 5'-CAG-3'/5'-CAG-3' was strongly bound to NA with a Ka of $1.8 \times 10^6\ M^{-1}$, whereas the A–A mismatch in 5'-GAC-3'/5'-GAC-3' was not as strongly bound. The observed sequence selectivity for ND- and NA-binding was most likely due to the stacking stabilization of the hydrogen-bonded heterocycles of MBL by the flanking base pairs, and also by direct hydrogen bonding of the heterocycles to the flanking bases. To look at the binding of damND to C–C, C–T, and T–T mismatches flanked by all possible combinations of base pairs, the duplexes used for SPR analyses contained the 5'-XNY-3'/5'-X'N'Y'-3' sequence, where N–N' represented C–C, C–T, T–T, G–G, and A–A mismatches, whereas X–Y' and Y–X' were Watson–Crick base pairs (Chart 1). Due to the local symmetry of the C–C, T–T, G–G, and A–A mismatches, the total number of DNA sequences examined was 56. In this series, the influence exerted by the second set of base pairs from the mismatched base pair on MBL-binding was not examined, because such a study require 16 times the number of sequences than that used here. The fully matched 27-mer duplexes did not produce any significant SPR signals on any of the three MBL surfaces studied.

2.4. SPR analyses

SPR measurements were performed by injecting DNA samples for 180 s to the three-MBL sensor to observe the association of the duplexes to the surface followed by a buffer flow in order to observe the dissociation of the bound DNA from the surface. The SPR response curves of each measurement were generated from 0 s (100 s before DNA injection) to 500 s (220 s after stopping DNA injection). The SPR response curves for C–C mismatches, C–T mismatches, T–T mismatches, G–G mismatches, and A–A mismatches are shown in Figure 3(a–e), respectively.

As expected from previous studies, the damND-immobilized surface produced marked SPR signals for all DNA duplexes containing C–C mismatches, whereas ND- and NA-immobilized surfaces produced only weak signals (Fig. 3a). Under the present sensor surface conditions and a DNA concentration of 1 μM, all C–C mismatched duplexes produced SPR signals of approximately 800 RU or larger. The shapes of the SPR response curves were similar for all C–C mismatches regardless of the base pairs flanking the mismatch. To evaluate the characteristics of DNA-binding to the MBL-immobilized surface, the ratio (RU_{500}/RU_{280}) of the SPR signal at 280 s (RU_{280}), where the signal reached maximum intensity, and that at 500 s (RU_{500}) was plotted against RU_{280} (Fig. 4a). In the scatter-plot of RU_{500}/RU_{280} against RU_{280} values, the affinity of the C–C mismatches to the surface was determined by the magnitude of RU_{280}, whereas the RU_{500}/RU_{280} ratio represented the rate of dissociation (k_d). In general, the dissociation constant (K_D) of the analyte to the surface could be determined from the SPR response curves, provided the binding stoichiometry was clarified, and this value was used for the analyte binding comparison. In a previous paper describing amND-binding to C–C mismatched duplexes, we analyzed K_D values by estimating the 1:1 binding stoichiometry for all duplexes. Sensors having a high ligand density on the surface, which were used in this study, are suitable for the detection of the analyte at low concentrations, whereas those having a low number of ligands on the surface are recommended for kinetic analysis. With the sensor surfaces that had a high ligand density, the degree of binding is probably controlled by the rate of mass transport of the analyte from the bulk solution to the surface[52] and the binding of the analyte to the surface may involve more than one ligand. To address the binding affinity of a different MBL to a large number of mismatched DNAs, we avoided an estimation-based discussion of the binding characteristics by using RU_{280} and the RU_{500}/RU_{280} ratio, which provided a qualitative comparison of the binding of analytes to the surface. The scatter-plot of RU_{500}/RU_{280} against RU_{280} clearly revealed that the RU_{500}/RU_{280} ratios remained within a very narrow range (0.42–0.54) for the binding of C–C mismatches to the damND surface. With the exception of 5'-GCC-3'/5'-GCC-3', which showed the lowest affinity, the RU_{280} ratio remained almost constant (0.48–0.54). To compare the damND-immobilized surface with the surface bearing the parent MBL amND,[38] the RU_{500}/RU_{280} ratio of the SPR data reported in a previous paper was calculated and plotted (Fig. 4f). While the signal intensities in Figure 4a and f could not be compared due to different amounts of damND and amND immobilized on the sensor surface, the scatter plots clearly demonstrated that the RU_{500}/RU_{280} ratio obtained for the amND-immobilized surface differed from that of the damND-immobilized surface; moreover, a wide-over distribution (0.11–0.37) was observed. The RU_{500}/RU_{280} ratio for the amND-immobilized surface was smaller than that for the damND-immobilized surface, which indicated that the dissociation of the bound C–C mismatched duplexes occured at a much faster rate on the amND-immobilized surface. These observations revealed that damND to C–C mismatches was much less sensitive to the base pair flanking the mismatch compared to the binding of amND.

Marked SPR signals against C–T mismatches were observed with the damND-immobilized surface, but this was not at all the case with the NA-immobilized surface (Fig. 3b). Weak affinity of the ND-immobilized surface was observed for some C–T mismatches. The SPR responses against C–T mismatches obtained with the damND surface were much more affected by the base pair flanking the mismatch than those against C–C mismatches, but the shapes of the SPR response curves were similar. The RU_{500}/RU_{280} plot (Fig. 4b) revealed these characteristics of the damND-immobilized surface in response to the C–T mismatches. The RU_{280} plots showed a wide-ranging distribution (146–495 RU), indicative of sequence-dependent affinity, but the RU_{500}/RU_{280} ratio remained within a narrow range (0.29–0.46), thereby demonstrating that the dissociation rate was not affected by the base pair flanking the mismatch.

The SPR response of the damND-immobilized surface to T–T mismatches showed marked sequence dependency (Fig. 3c). Among 10 sequences, two T–T mismatches in the 5'-GTC-3'/5'-CTG-3' and 5'-GTA-3'/5'-CTT-3' sequences yielded a strong SPR signal, whereas modest-intensity SPR signals were observed for the eight remaining T–T mismatches. The RU_{500}/RU_{280} values clearly fell into two groups (Fig. 4c), that is, high RU_{280} values (~1100 RU) with high RU_{500}/RU_{280} ratios (~0.7), and low RU_{280} (62–310 RU) values with RU_{500}/RU_{280} ratios (0.32–0.47) comparable to

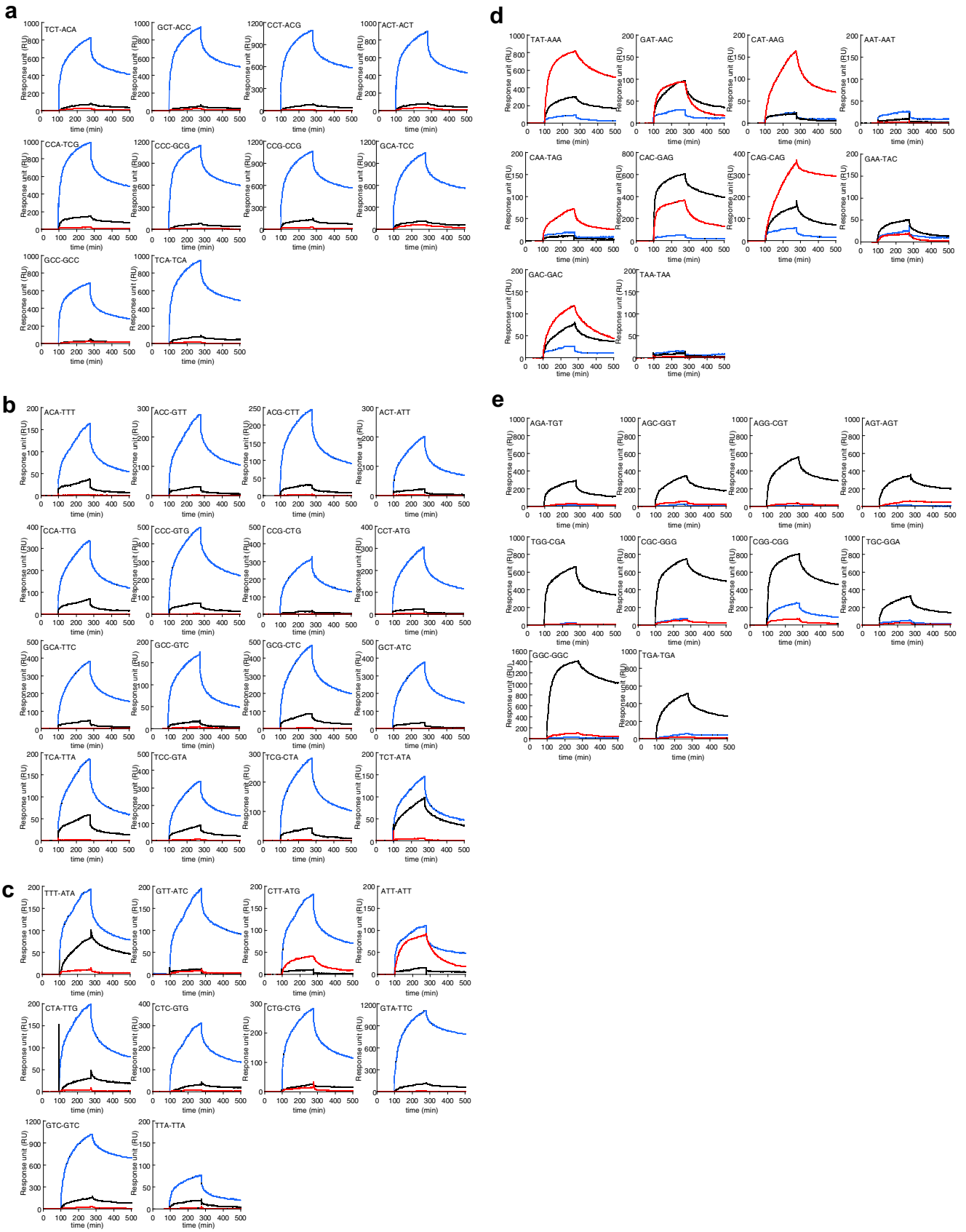

Figure 3. SPR response curves of DNA duplexes containing (a) C–C mismatches in the 5'-XCY-3'/5'-X'CY'-3' sequence, (b) C–T mismatches in the 5'-XCY-3'/5'-X'TY'-3' sequence, (c) T–T mismatches in the 5'-XTY-3'/5'-X'TY'-3' sequence (d) A–A mismatches in the 5'-XGY-3'/5'-X'GY'-3' sequence, and (e) G–G mismatches in the 5'-XAY-3'/5'-X'AY'-3' sequence analyzed with three MBL sensors. SPR response curves are shown from 0 s to 500 s. The sensors were exposed to the DNA sample for 100–280 s. For the sake of clarity, the scale of the *Y*-axis varied with measurements. Key: damND surface, blue; ND surface, black; NA surface, red.

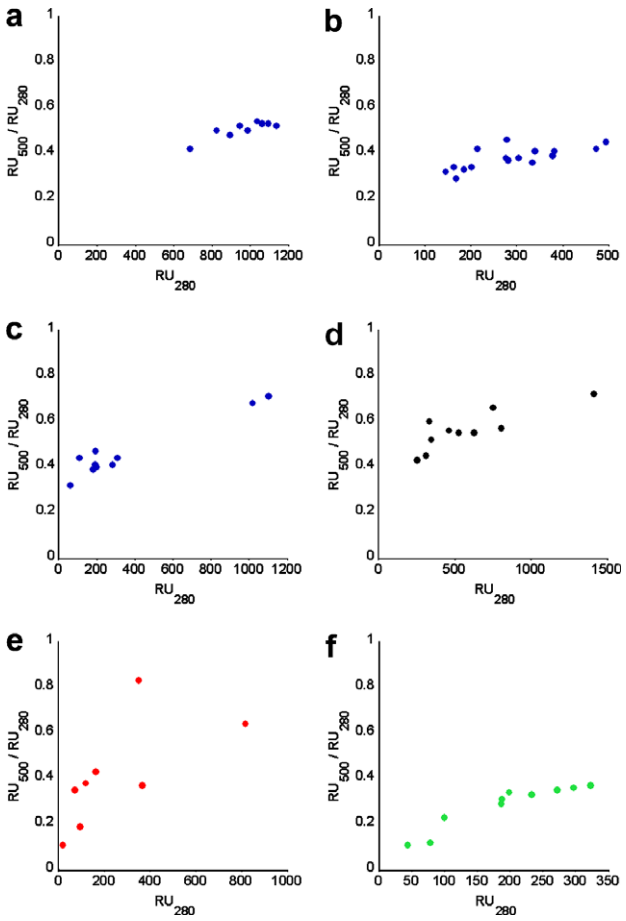

Figure 4. Scatter-plots of RU500/RU280 against RU280 for (a) C–C, (b) C–T, (c) T–T mismatches on a damND-immobilized sensor; (d) G–G mismatches on an ND-immobilized sensor; (e) A–A mismatches on an NA-immobilized sensor; and (f) C–C on an amND-immobilized sensor.

those obtained for C–T mismatches. These results strongly suggested that the mode of damND binding to 5'-GTC-3'/5'-GTC-3' and 5'-GTA-3'/5'-TTC-3' sequences differs from that to other T–T mismatches. Detailed analyses of damND-binding to these two types of T–T mismatch are now ongoing, and will be reported separately. The ND-immobilized surface exhibited affinity for 5'-TTT-3'/5'-ATA-3', whereas the NA-immobilized surface showed affinity for 5'-ATT-3'/5'-ATT-3'; however, neither of these two surfaces interacted significantly with other T–T mismatches.

As a summary, the damND-immobilized surface showed (1) sequence-independent affinity for C–C mismatches, with a similar dissociation rate in each case, (2) sequence-dependent affinity for C–T mismatches and a similar dissociation rate in each case, and (3) sequence-dependent affinity and dissociation rate for T–T mismatches. These characteristic features were clearly noticed by comparing the ND- and NA-immobilized surfaces. The ND-immobilized surface exhibited a sequence-dependent affinity for G–G mismatches (Fig. 3d). The RU_{500}/RU_{280} ratio was distributed across a wide range of values (0.43–0.72), indicating that the dissociation rate was also sequence-dependent (Fig. 4d). This sequence-dependent binding of an ND-immobilized surface to G–G mismatches is fully consistent with our previous observations. The NA-immobilized surface yielded a markedly different scatter-plot from those obtained with damND- and ND-immobilized surfaces (Fig. 3e). The plot was completely disordered, showing a wide distribution of both RU_{280} (19–817 RU) and RU_{500}/RU_{280} (0.11–0.90) values (Fig. 4e). The present observation of highly sequence-dependent NA-binding to A–A mismatches is fully supported by our previous results from thermal denaturation studies of A–A mismatches in the presence of NA.

3. Conclusion

A new MBL, damND, was synthesized and immobilized on an SPR sensor surface. The damND-immobilized surface showed improved binding to C–C mismatches in terms of both affinity and sequence dependency, as compared to a surface bearing the parent compound, amND. The damND-immobilized surface was found to be effective at identifying C–T and T–T mismatches in a sequence-dependent manner. As regards detecting mismatched duplexes, the damND-immobilized surface complemented the features of ND- and NA-immobilized surfaces, which exhibit affinity for mismatches composed of purine nucleotide bases. Thus, SPR sensor surfaces simultaneously bearing three MBLs, (ND, NA, and damND) are expected to be useful for detecting mismatches in duplex DNA.

4. Experimental

4.1. General

Reagents and solvents were purchased from standard suppliers and used without further purification. Oligodeoxynucleotides were purchased from Gene Design. ^{1}H NMR spectra were measured with Varian Mercury 400 (400 MHz) spectrometer. ^{13}C NMR spectra were measured with JEOL JMN 500 α-500(125 MHz) spectrometer. Coupling constants (*J* value) were reported in Hertz. The chemical shifts are expressed in ppm downfield from tetramethylsilane, using residual chloroform (δ = 7.24 in ^{1}H NMR, δ = 77.0 in ^{13}C NMR), and methanol (δ = 3.30 in ^{1}H NMR, δ = 49.0 in ^{13}C NMR), as an internal standard. FAB mass spectra were recorded on JEOL JMS HX-110 spectrometer. Absorption spectra measurements were carried out using SHIMADZU UV-2550 UV–vis spectrometer.

4.2. *N*-(*N*'-Boc-3-aminopropyl)-2,7-diamino-1,8-naphthyridine (2)

To a solution of *N*-acethyl-2-amino-7-chloro-1,8-naphthyridine (3.31 g, 16 mmol) in chloroform (10 mL) in a sealed tube, *N*-Boc-1,3-diaminopropane (5.1 g, 29 mmol) was added. The mixture was heated at 120 °C for two days. After cooling, the mixture was concentrated in vacuo and the residue was diluted with chloroform and washed with $NaHCO_3$. The organic solution was dried over Na_2CO_3, filtered, and concentrated in vacuo. The residue was purified by silica gel column chromatography (2–5% $CHCl_3$ in MeOH) to give **2** (3.03 g, 58%); ^{1}H NMR ($CDCl_3$) δ = 7.62 (d, 1 H, *J* = 8.4 Hz), 7.56 (d, 1 H, *J* = 8.4 Hz), 6.45 (d, 1 H, *J* = 8.4 Hz), 6.42 (d, 1 H, *J* = 8.4 Hz), 3.49 (t, 2 H, *J* = 6.8 Hz), 3.14 (t, 2 H, *J* = 6.8 Hz), 1.78 (quint, 2 H, *J* = 6.8 Hz), 1.42 (s, 9H); ^{13}C NMR ($CDCl_3$) δ = 161.9, 161.3, 158.6, 158.0, 139.1, 137.9, 111.4, 109.0, 107.5, 79.9, 39.4, 39.1, 30.8, 28.8; FABMS (NBA), *m/e* 318 [$(M+H)^+$]; HR-FABMS calcd for $C_{16}H_{23}N_5O_2$ [$(M+H)^+$] 318.1930, found 318.1949.

4.3. *N*-(3-Aminopropyl)-2,7-diamino-1,8-naphthyridine (3)

To a solution of **2** (0.37 g, 1.2 mmol) in chloroform (10 mL), 4 N HCl in ethyl acetate (4 mL) was added, and the mixture was stirred at room temperature for 30 min. The organic solvent was removed under reduced pressure. DOWEX HO^- was added to the residue, and the mixture was diluted with 50% methanol in water (10 mL). The mixture was then filtrated, and the filtrate was co-evaporated with pyridine (2× 1 mL), toluene (2× 1 mL), ethanol

(2× 1 mL), and finally with chloroform to give **3** (0.25 g, 98%); ^{1}H NMR ($CDCl_3$) δ = 7.57 (d, 1 H, J = 8.8 Hz), 7.51 (d, 1H, J = 8.4 Hz), 6.43 (d, 1H, J = 8.4 Hz), 6.39 (d, 1 H, J = 8.8 Hz), 3.51 (t, 2H, J = 6.8 Hz), 2.66 (t, 2 H, J = 6.8 Hz), 1.73 (quint, 2 H, J = 6.8 Hz); ^{13}C NMR (CD_3OD) δ = 160.8, 155.7, 148.5, 142.7, 136.8, 110.1, 108.4, 105.8, 37.1, 36.9, 27.2; FABMS (NBA), m/e 218 [(M+H)$^+$]; HR-FABMS calcd. for $C_{11}H_{16}N_5$ [(M+H)$^+$] 218.1406, found 218.1406.

4.4. *N*-Boc-damND (4)

A suspension of **3** (0.25 g, 1.2 mmol) in DMSO (6 mL) was sonicated for a few minutes and *N*-Boc-3,3-iminobis(pentafluorophenyl propionate) (0.27 g, 0.46 mmol) was added. The whole mixture was further sonicated for 5 min to give a clear solution. TLC monitoring of the reaction revealed completion of the coupling. The solution was diluted with ethyl ether and washed with $NaHCO_3$. The organic layer was discarded and the aqueous layer was washed with ethyl acetate. The aqueous layer was extracted with chloroform. The organic layer was dried over Na_2SO_4, filtered, and concentrated *in vacuo*. The product was purified by preparative TLC to give **4** (0.24 g, 79% based on the linker); ^{1}H NMR (CD_3OD) δ = 7.61 (d, 1 H, J = 8.4 Hz), 7.55 (d, 1 H, J = 8.4 Hz), 6.44 (d, 1 H, J = 8.8 Hz), 6.41 (d, 1 H, J = 8.4 Hz), 3.52 (t, 4 H, J = 6.8 Hz), 3.49 (t, 4 H, J = 6.8 Hz), 3.25 (br, 4 H), 2.48 (br, 4 H), 1.78 (br t, 4 H, J = 6.4 Hz), 1,41 (s, 9H); ^{13}C NMR (CD_3OD) δ = 172.7, 160.8, 160.2, 156.8, 155.9, 137.9, 136.7, 110.2, 107.8, 106.4, 80.2, 78.3, 44.4, 38.0, 36.8, 29.3, 27.5; FABMS (NBA), m/e 660 [(M + H)$^+$]; HR-FABMS calcd for $C_{33}H_{45}N_{11}O_4$ [(M + H)$^+$] 660.3734, found 660.3734.

4.5. *N*-Boc-linker-damND (5)

To a solution of **4** (99 mg, 0.15 mmol) in methanol (5 mL) 4 N HCl in ethyl acetate (2 mL) was added, and the mixture was stirred at room temperature for 1 h. The solution was concentrated in vacuo. The residue was co-evaporated with chloroform (1 mL) and then with methanol (1 mL) to give damND **1**, which was used in the next step without further purification. To the solution of crude **1** in 10 mL MeOH, 4-((*tert*-butoxy)carobnylamino)-*N*-(3'-oxopropyl)butanamide (127 mg, 0.5 mmol), and then $NaBH_3CN$ (19 mg, 0.3 mmol) in 300 μL MeOH were added. The pH of the solution was adjusted to approximately 4 by the addition of Et_3N and acetic acid. The mixture was stirred for 2 h at room temperature. The reaction mixture was diluted with chloroform and washed with $NaHCO_3$. The organic phase was dried over Na_2SO_4, filtered, and concentrated *in vacuo*. The product was purified by silica gel column chromatography ($CHCl_3$/MeOH) to give **5** (86 mg, 71% 2 steps); 7.60 (d, 2 H, J = 8.4 Hz), 7.54 (d, 2 H, J = 8.8 Hz), 6.44 (d, 2 H, J = 8.4 Hz), 6.40 (d, 2 H, J = 8.4 Hz), 3.48 (t, 4 H, J = 6.4 Hz), 3.24 (t, 4 H, J = 6.8 Hz), 3.11 (t, 2 H, J = 7.2 Hz), 3.01 (t, 2 H, J = 7.2 Hz), 2.73 (t, 4 H, 6.4 Hz), 2.45 (t, 2 H, J = 7.6 Hz), 2.38 (t, 4 H, J = 6.4 Hz), 2.14 (t, 2 H, J = 7.6 Hz), 1.77 (quint, 4 H, J = 6.4 Hz), 1.70 (tt, 2 H, J = 7.6, 7.2 Hz), 1.60 (quint, 2 H, J = 7.2 Hz), 1.40 (s, 9 H); ^{13}C-NMR (CD_3OD) δ = 174.3, 173.9, 160.8, 160.2, 156.8, 137.9, 136.8, 110.3, 107.9, 106.4, 78.8, 78.3, 50.8, 49.9, 39.7, 38.1, 37.5, 36.7, 35.6, 33.2, 29.2, 27.6, 26.6, 26.2; FABMS (NBA), m/e 802 [(M + H)$^+$]; HR-FABMS calcd for $C_{40}H_{60}N_{13}O_5$ [(M + H)$^+$] 802.4840, found 802.4839.

4.6. Preparation of damND-immobilized surface

Surface plasmon resonance measurements were performed with a BIAcore 2000 system (BIAcore, Uppsala, Sweden). Immobilization of MBL on a CM5 sensor chip (carboxymethylated dextran surface, BIAcore) was carried out using an amine coupling kit (BIAcore) under a continuous flow of HBS-N buffer (10 mM HEPES, pH 7.4) containing NaCl (150 mM) at a flow rate of 10 μL/min. A solution (70 μL) of *N*-hydroxysuccinimide (0.05 M) and 1-(3-dimethylaminopropyl)-3-ethylcarbodiimide hydrochloride (0.2 M) was injected using the QUICKINJECT command to activate the carboxymethylated dextran surface of the CM5 sensor chip. A solution (70 μL) of crude **6** (2 mM in borate buffer, pH 9.2) prepared by deprotection of **5** with 4N HCl (as described for the preparation of **1**) was injected using the QUICKINJECT command on the activated surface. Residual activated surface was completely blocked by injection of a solution (20 μL) of ethanolamine hydrochloride (1.0 M, pH 8.5). Non-covalently bound material was removed by washing with 5 μL of 50 mM NaOH to produce the sensor chip carrying damND on its surface. The amount of damND immobilized on the surface was modulated by the duration of the immobilization reaction period, and was monitored as an increase in the SPR signal (RU, resonance units) after deactivation of the unreacted NHS-esters and conditioning of the surface. Immobilization of ND and NA in different flow channels of the same sensor was carried out as described above.

4.7. SPR Measurements

All measurements were carried out at 25 °C under the continuous flow of a buffer (10 mM HEPES, pH 7.4) containing NaCl (0.5 M) at a flow rate of 30 μL/min. After the surface had been conditioned by 100 sec exposure to the buffer flow, a 1 μM solution of 27-mer duplexes in buffer were injected for 180 sec to analyze association to the sensor surface. The buffer was subsequently injected for another 220 sec in order to determine the dissociation of the bound oligomer from the surface. After each analysis, all binding materials were removed by washing the sensor surfaces with 30 μL of NaOH solution (50 mM). Immediately after being washed, the system was prepared for use in a subsequent assay.

Acknowledgements

This work was supported by Grant in Aid for Scientific Research (S) (18105006) and (B) (18750147) from the Japan Society for the Promotion of Science (JSPS).

References and notes

1. Collins, E.; Green, E. D.; Guttmacher, A. E.; Guyer, M. S. *Nature* **2003**, *422*, 835.
2. Evans, W. E.; Relling, M. V. *Nature* **2004**, *429*, 464.
3. Kruglyak, L.; Nickerson, D. A. *Nat. Genet.* **2001**, *27*, 234.
4. Hirschhorn, J. N.; Daly, M. J. *Nat. Rev. Genet.* **2005**, *6*, 95.
5. Syvänen, A.-C. *Nat. Rev. Genet.* **2001**, *2*, 930.
6. Nakatani, K. *Chembiochem* **2004**, *12*, 1623.
7. Metzker, M. L. *Genome Res.* **2005**, *15*, 1767.
8. Nyrén, P.; Lundin, A. *Anal. Biochem.* **1985**, *151*, 504.
9. Ronaghi, M.; Uhlén, M.; Nyrén, P. *Science* **1998**, *281*, 363.
10. Tyagi, S.; Kramer, F. R. *Nat. Biotechnol.* **1996**, *14*, 303.
11. Howell, W. M.; Jobs, M.; Gyllensten, U.; Brookes, A. J. *Nat. Biotechnol.* **1999**, *17*, 87.
12. Hacia, J. G. *Nat. Genet.* **1999**, *21*, 42.
13. Whitcombe, D.; Theaker, J.; Guy, S. P.; Brow, T.; Little, S. *Nat. Biotechnol.* **1999**, *17*, 804.
14. Yamane, A. *Nucleic Acids Res.* **2002**, *30*, e97.
15. Hwang, G. T.; Seo, Y. J.; Kim, B. H. *J. Am. Chem. Soc.* **2004**, *126*, 6528.
16. Seo, Y. J.; Ryu, J. H.; Kim, B. H. *Org. Lett.* **2005**, *7*, 4931.
17. Yamana, K.; Fukunaga, Y.; Ohtani, Y.; Sato, S.; Nakamura, M.; Kim, W. J.; Akaike, T.; Maruyama, A. *Chem. Commun.* **2005**, 2509.
18. Kchler, O.; Jarikote, D. V.; Seitz, O. *ChemBioChem* **2005**, *6*, 69.
19. Silverman, A. P.; Kool, E. T. *Nucleic Acids Res.* **2005**, *33*, 4978.
20. Valis, L.; Amann, N.; Wagenknecht, H.-A. *Org. Biomol. Chem.* **2005**, *3*, 36.
21. Bethge, L.; Jarikote, D. V.; Seitz, O. *J. Med. Chem.* **2008**, *16*, 114.
22. Lukhtanov, E. A.; Lokhov, S. G.; Gorn, V. V.; Podyminogin, M. A.; Mahoney, W. *Nucleic Acids Res.* **2007**, *35*, e30.
23. Tainaka, K.; Tanaka, K.; Ikeda, S.; Nishiza, K.; Unzai, T.; Fujiwara, Y.; Saito, I.; Okamoto, A. *J. Am. Chem. Soc.* **2007**, *129*, 4776.
24. Okamoto, A.; Kanatani, K.; Saito, I. *J. Am. Chem. Soc.* **2004**, *126*, 4820.
25. Okamoto, A.; Saito, Y.; Saito, I. *J. Photochem. Photobiol. C* **2005**, *6*, 108.
26. Litos, I. K.; Ioannou, P. C.; Christopoulous, T. K.; Traeger-Synodinos, J.; Kanavakis, E. *Anal. Chem.* **2007**, *79*, 395.

27. Pastinen, T.; Kurg, A.; Metspalu, A.; Peltonen, L.; Syvanen, A. C. *Genome Res.* **1997**, *7*, 606.
28. Newton, C. R.; Graham, A.; Heptinstall, L. E.; Powell, S. J.; Summers, C.; Kalsheker, N.; Smith C, J.; Markham, A. F. *Nucleic Acids Res.* **1989**, *17*, 2503.
29. Gibbs, R. A.; Nguyen, P. N.; Caskey, C. T. *Nucleic Acids Res.* **1989**, *17*, 2437.
30. Germer, S.; Holland, M. J.; Higuchi, R. *Genome Res.* **2000**, *10*, 258.
31. Wu, D. Y.; Ugozzoli, L.; Pal, B. K.; Wallace, R. B. *Proc. Natl. Acad. Sci. USA* **1989**, *86*, 2757.
32. Shively, L.; Chang, L.; LeBon, J. M.; Liu, Q.; Riggs, A. D.; Singer-Sam, J. *Biotechniques* **2003**, *34*, 498.
33. Guo, Z.; Liu, Q. H.; Smith, L. M. *Nat. Biotechnol.* **1997**, *15*, 331.
34. Jackson, B. A.; Barton, J. K. *J. Am. Chem. Soc.* **1997**, *119*, 12986.
35. Jackson, B. A.; Alekseyev, V. Y.; Barton, J. K. *Biochemistry* **1999**, *38*, 4655.
36. Lacy, E. R.; Cox, K. K.; Wilson, W. D.; Lee, M. *Nucleic Acids Res.* **2002**, *30*, 1834.
37. Nakatani, K.; Sando, S.; Saito, I. *Nat. Biotechnol.* **2001**, *19*, 51.
38. Nakatani, K.; Sando, S.; Kumasawa, H.; Kikuchi, J.; Saito, I. *J. Am. Chem. Soc.* **2001**, *123*, 12650.
39. Nakatani, K.; Kobori, A.; Kumasawa, H.; Saito, I. *Bioorg. Med. Chem. Lett.* **2004**, *14*, 1105.
40. Peng, T.; Murase, T.; Goto, Y.; Kobori, A.; Nakatani, K. *Bioorg. Med. Chem. Lett.* **2005**, *15*, 259.
41. Hagihara, S.; Kumasawa, H.; Goto, Y.; Hayashi, G.; Kobori, A.; Saito, I.; Nakatani, K. *Nucleic Acids Res.* **2004**, *32*, 278.
42. Nakatani, K.; Hagihara, S.; Sando, S.; Sakamoto, S.; Yamaguchi, K.; Maesawa, C.; Saito, I. *J. Am. Chem. Soc.* **2003**, *125*, 662.
43. Myers, R. M.; Larin, Z.; Maniatis, T. *Science* **1985**, *230*, 1242.
44. Fazakerley, G. V.; Qignard, E.; Woisard, A.; Guschlbauer, W.; van der Marel, G. A.; van Boom, J. H.; Jones, M.; Radman, M. *EMBO. J.* **1986**, *5*, 3697–3703.
45. Beijer, F. H.; Kooijman, H.; Spek, A. L.; Sijbesma, R. P.; Meijer, E. W. *Angew. Chem. Int. Ed.* **1987**, *37*, 75.
46. Kobori, A.; Horie, S.; Suda, H.; Saito, I.; Nakatani, K. *J. Am. Chem. Soc.* **2004**, *126*, 557.
47. Suda, H.; Kobori, A.; Zhang, J.; Hayashi, G.; Nakatani, K. *Bioorg. Med. Chem.* **2005**, *13*, 4507.
48. Park, T.; Mayer, M. F.; Nakashima, S.; Zimmerman, S. C. *Synlett* **2005**, *9*, 1435.
49. Corbin, P. S.; Zimmerman, S. C.; Thiessen, P. A.; Hawryluk, N. A.; Murray, T. J. *J. Am. Chem. Soc.* **2001**, *123*, 10475.
50. Pharmacia-Biosensor. **1990** Biacore User's Manual. Piscatway, NJ.
51. Löfås, S.; Johnson, B. *J. Chem. Soc. Chem. Commun.* **1990**, *21*, 1526.
52. Stenberg, M.; Nygren, H. J. *Theor. Biol.* **1985**, *113*, 129.